OPEN ACCESS
Fractals, Vol. 28, No. 8 (2020) 2040007 (13 pages)

DOI: 10.1142/S0218348X20400071

PIECEWISE OPTIMAL FRACTIONAL REPRODUCING KERNEL SOLUTION AND CONVERGENCE ANALYSIS FOR THE ATANGANA–BALEANU–CAPUTO MODEL OF THE LIENARD'S EQUATION

SHAHER MOMANI,[*,†,§] OMAR ABU ARQUB[‡,¶] and BANAN MAAYAH[†,‖]
[*]*Department of Mathematics and Sciences, College of Humanities and Sciences Ajman University, Ajman, UAE*
[†]*Department of Mathematics, Faculty of Science The University of Jordan Amman 11942, Jordan*
[‡]*Department of Mathematics, Faculty of Science Al-Balqa Applied University Salt 19117, Jordan*
[§]*s.momani@ajman.ac.ae; s.momani@ju.edu.jo*
[¶]*o.abuarqub@bau.edu.jo*
[‖]*b.maayah@ju.edu.jo*

Received January 5, 2020
Accepted March 5, 2020
Published July 10, 2020

Abstract

In this paper, an attractive reliable analytical technique is implemented for constructing numerical solutions for the fractional Lienard's model enclosed with suitable nonhomogeneous initial conditions, which are often designed to demonstrate the behavior of weakly nonlinear waves arising in the oscillating circuits. The fractional derivative is considered in the Atangana–Baleanu–Caputo sense. The proposed technique, namely, reproducing kernel Hilbert space method,

[¶]Corresponding author.

optimizes numerical solutions bending on the Fourier approximation theorem to generate a required fractional solution with a rapidly convergent form. The influence, capacity, and feasibility of the presented approach are verified by testing some applications. The acquired results are numerically compared with the exact solutions in the case of nonfractional derivative, which show the superiority, compatibility, and applicability of the presented method to solve a wide range of nonlinear fractional models.

Keywords: Atangana–Baleanu–Caputo Fractional Derivative; Fractional Lienard's Model; Piecewise Optimal Fractional Reproducing Kernel Method.

1. PREFACE AND PRESENTATION

Mathematical simulation of nonlinear physical and abstract models is a very vital process for predicting the solution behavior of fractional differential equations (FDEs) corresponding to different applications in science and engineering, While computational models of physical systems are typically triggered through computer simulations, symbolic programming, and approximate numerical algorithms for emerging nonlinear problems, which often include a set of corresponding FDEs. Solutions of such nonlinear FDEs issues are great importance for describing the dynamic and asymptotic behaviors of materials in many applications such as electric circuit, fluid mechanics, viscoelastic damping, electromagnetic, and electrochemistry.[1–5] In this light, there exists no classic, precise method that yields an analytical solution within a closed form in terms of spatial and temporal parameters to deal with these types of nonlinear evolution models. Therefore, there is an urgent need for effective and sophisticated methods and algorithms for exploring analytical solutions of such challenges.

The fractional calculus approach is a powerful generalization of the classical calculus that deals with real order differentiation and integration. Recently, it has been extensively examined as an excellent tool in describing genetic properties, memory effort, and material transfer mechanisms in many connected areas of engineering and applied sciences.[6–13] Unlike classical calculus, which has a unique definition and clear geometrical and physical interpretations, there are many definitions for the fractional operations, including Riemann–Liouville, Caputo, Riesz, and Grünwald–Letnikov.[1–5] In view of this, a novel concept of fractional calculus, namely the Atangana–Baleanu–Caputo (ABC) fractional derivative, has been proposed in Ref. 14. Since then several studies have appeared in the literature, for more details see Refs. 15–25. Supplementary, this fractional ABC derivative seems to be liberating of singularity with local kernel function, because the kernel depends on the exponential formulation. Aught, this definition is elaborated upon with its special properties strongly and heavily in recent times as utilized in Refs. 14–25.

In the current work, the application of the piecewise optimal fractional reproducing kernel method (FRKM) is extended to provide a convenient methodology to derive approximate numerical solution for model of the fractional Lienard's equation (FLE) arising in oscillating circuits with ABC derivative. To achieve our goal, we consider the subordinate model:

$$\begin{cases} {}_0^{ABC}\partial_t^{\delta}\mu(t) + \lambda(\mu(t))\,\partial_t\mu(t) + \eta(\mu(t)) = \gamma(t), \\ \mu(0) = \rho, \\ \partial_t\mu(0) = \rho'. \end{cases} \tag{1}$$

To assign more on model of the FLE: $\lambda(\mu(t))\,\partial_t\mu(t)$ indicates the damping force, $\eta(\mu(t))$ denotes the restoring force, and $\gamma(t)$ stands for the external force. In the development of radio and vacuum tube technology, FLE is extremely investigated to describe the oscillating circuits. In reality, the FLE contains the damped pendulum or a damped spring–mass system as a particular case. It is also very useful as nonlinear models of various scientific fields while considering various selection of $\lambda(\mu(t))$, $\eta(\mu(t))$, and $\gamma(t)$. For paradigm, the choice $\lambda(\mu(t)) = a(\mu^2(t) - 1)$, $\eta(\mu(t)) = \mu(t)$, and $\gamma(t)$ progresses to Eq. (1) to the fractional Van der Pol equation used as a nonlinear model of electronic oscillation. More details about elaborated investigations of FLE model with its special properties one can refer to Refs. 26–30.

Extremely, we will symbolize the following: $\mathbb{I} := [0,1]$; $\delta \in (1, 2]$; $\rho\rho' \in \mathbb{R}$; $\lambda\eta \in \mathcal{C}(\mathbb{R},\mathbb{R})$; and μ, $\gamma \in \mathcal{C}(\mathbb{I},\mathbb{R})$. Exceedingly, we will write ${}_0^{ABC}\partial_t^{\delta}\mu(t)$

to sign the ABC fractional derivative of μ in t over $\mathbb{A}$ of order δ and is realized as

$$ {}_0^{ABC}\partial_t^{\delta}\mu(t) = \frac{1-\delta+\delta\Gamma^{-1}(\delta)}{1-\delta} \int_0^t \partial_t^2\mu(\tau)\, M_\delta\left(-\frac{\delta}{1-\delta}(t-\tau)^\delta\right) d\tau, \quad (2)$$

in which $t = 0$ is a base point acquaint at $t \in \mathbb{I} - \{0,1\}$ and $\mathfrak{u} \in \Upsilon^2(\mathbb{I} - \{0,1\})$. However, $M_\delta(t) = \sum_{n=0}^{\infty}(1/\Gamma(n\delta+1))t^n$ with $\delta > 0$ and $t \in \mathbb{R}$ is the Mittag-Leffler function and Υ^2 is the Sobolev space of order 2 on the domain $\mathbb{I} - \{0,1\}$ and is realized as

$$\Upsilon^2(\mathbb{I} - \{0,1\}) = \left\{\mu \in L^2(\mathbb{I} - \{0,1\}) : \partial_t\mu(t), \partial_t^2\mu(t) \in L^2(\mathbb{I} - \{0,1\})\right\}. \quad (3)$$

The standard RKM main area topic is in mathematical modeling and numerical simulation of multidimensional issues arising in engineering and physical sciences.[31–33] Later, the FRKM has been used in generating numerical solutions for strongly nonlinear integral–differential operators in the form of a rapidly convergent series with a minimum size of calculations without any restrictive hypotheses. So, this adaptive has been used as an alternative technique in solving several nonlinear and discontinuous shapes problems arising in engineering and physics as utilized in Refs. 34–39.

In addition to the preface and presentation cutter, the residual synopsis of the article is structured in the following subsidiary sections: preliminaries and assumptions in the FRKM: requirements, principles, and tools; impersonation solution of FLE in the ABC sense: formulation and solutions; convergence and error conductance: behavior and characterization theorems; numerical applications and computational results: FRKM steps, test applications, and discussions. Finally, summary and outline are utilized on record.

2. PRELIMINARIES AND ASSUMPTIONS IN THE FRKM

This section is dedicated to briefly present some definitions and properties of the FRKM and its corresponding hypothesis. At all events, the FRKM is an effective approach for solving wide class of differential–integral operators in the fractional emotion and provided a general numeric scheme to handle the solution behaviors. Extremely, we will symbolize $|\mathcal{C}(\mathbb{I})|$ to denote the set of absolutely continuous functions on $\mathbb{I}$.

Let $\mathcal{H}$ be a Hilbert space of functions defined on $\mathbb{A}$. A function $\Psi \in \mathrm{C}(\mathbb{I}\times\mathbb{I},\mathbb{R})$ is a reproducing kernel of $\mathcal{K}$ if it fulfills the subsequent requirements:

$$\begin{cases} \forall t \in \mathbb{I} : \Psi(\bullet, t) \in \mathcal{H}, \\ \forall \psi \in \mathcal{H} \text{ and } \forall t \in \mathbb{I} : \langle \psi(\cdot), \Psi(\cdot, t)\rangle_{\mathcal{H}} = \psi(t). \end{cases} \quad (4)$$

Definition 1 (Ref. 17). The Hilbert space $\mathcal{A}(\mathbb{I})$ and its functional structure are arranged as

$$\begin{cases} \mathcal{A}(\mathbb{I}) = \left\{\mu(t) : \mu(t), \partial_t\mu(t), \partial_t^2\mu(t) \in |\mathcal{C}(\mathbb{I})|; \partial_t^3\mu(t) \in L^2(\mathbb{I}); \mu(0) = \partial_t\mu(0) = 0\right\}, \\ \langle \mu(t), \nu(t)\rangle_{\mathcal{A}} = \sum_{i=0}^{2}\partial_t^i\mu(0)\,\partial_t^i\nu(0) + \int_{\mathbb{I}}\partial_t^3\mu(t)\,\partial_t^3\nu(t)\,dt, \\ \|\mu\|_{\mathcal{A}} = \sqrt{\langle \mu(t), \mu(t)\rangle_{\mathcal{A}}}. \end{cases} \quad (5)$$

Definition 2 (Ref. 17). The Hilbert space $\mathcal{B}(\mathbb{I})$ and its functional structure are arranged as

$$\begin{cases} \mathcal{B}(\mathbb{I}) = \left\{\mu(t) : \mu(t) \in |\mathcal{C}(\mathbb{I})|; \partial_t\mu(t) \in L^2(\mathbb{I})\right\}, \\ \langle \mu(t), \nu(t)\rangle_{\mathcal{B}} = \int_{\mathbb{I}} (\mu(t)\,\nu(t) + \partial_t\mu(t)\,\partial_t\nu(t))\,dt, \\ \|\mu\|_{\mathcal{B}} = \sqrt{\langle \mu(t), \mu(t)\rangle_{\mathcal{B}}}. \end{cases} \quad (6)$$

Theorem 1 (Ref. 17). *The Hilbert space $\mathcal{A}(\mathbb{I})$ is a complete reproducing kernel with kernel function*

$$\mathcal{M}_t(s) = \frac{1}{120}\begin{cases} s^2\left(-5s^2t + s^3 + 10t^2(3+s)\right), & s \le t, \\ t^2\left(-5t^2s + t^3 + 10s^2(3+t)\right), & s > t. \end{cases} \quad (7)$$

Theorem 2 (Ref. 17). *The Hilbert space $\mathcal{B}(\mathbb{I})$ is a complete reproducing kernel with kernel function*

$$\mathcal{N}_t(s) = \frac{1}{2}\mathrm{csch}(1) \begin{cases} \cosh(t+s-1) + \cosh(t-s-1), & s \le t, \\ \cosh(t+s-1) + \cosh(s-t-1), & s > t. \end{cases} \quad (8)$$

In the applicability of the FRKM, we divide the compact set $\mathbb{I}$ into uniform splits encoded by t_i. This assumed that the gained set $\{t_i\}_{i=1}^{\infty}$ will be dense in $\mathbb{I}$. Anyhow, we attempt to cover the set as well as the numerical process should end up in finite phases.

For independency, if $\{\sigma_i\}_{i=1}^{m}$ is fixed according to $\sum_{i=1}^{m}\sigma_i\mathcal{M}_{t_i}(s) = 0$, takeover $h_k(s) \in \mathcal{A}(\mathbb{I})$ as to $h_k(s_l) = \delta_{l,k}, \forall l = 1, 2, \ldots m$, then $0 = \langle h_k(s),$

$\sum_{i=1}^{m} \sigma_i \mathcal{M}_{t_i}(s)\rangle_{\mathcal{A}} = \sum_{i=1}^{m} \sigma_i \langle h_k(s), \mathcal{M}_{t_i}(s)\rangle_{\mathcal{A}} = \sum_{i=1}^{m} \sigma_i h_k(s_i) = \sigma_i$ for $k = 1, 2, \ldots m$. De facto, this showed that $\{\mathcal{M}_{t_i}(s)\}_{i=1}^{m}$ is linearly independent $\forall m \geq 1$. To generalize more, this will generate the subordinate result: the system $\{\mathcal{M}_{t_i}(s)\}_{i=1}^{\infty}$ is linearly independent in $\mathcal{A}(\mathbb{I})$.

3. IMPERSONATION SOLUTION OF FLE IN THE ABC SENSE

The main tools in the FRKM are as follows: building appropriate Hilbert spaces, generating corresponding kernel functions, defining appropriate differential linear operator, fitting orthonormal function systems, collecting symbolic computations and data sets, and software mathematical package solver. Hither, the FRKM is developing to construct highly efficient numerical solutions for the FLE that arise in the engineering and physical sciences and combine the implementations in a user-friendly framework.

Hither, based on applied the auxiliary parameterized technique and to fixed the suggested solution in $\mathcal{A}(\mathbb{I})$, the subsequent replacement $\mu(t) :\to \mu(t) - (\rho' t + \rho)$ will convert FLE of Eq. (1) into homogenous one. Anyhow, we still signify the conversion solution by $\mu(t)$ as

$$\begin{cases} {}_0^{ABC}\partial_t^{\delta}\mu(t) + \bar{\lambda}(\mu(t))\,\partial_t\mu(t) + \bar{\eta}(\mu(t)) = \bar{\gamma}(t), \\ \mu(0) = 0, \\ \partial_t\mu(0) = 0. \end{cases} \tag{9}$$

Essentially, define the linear operator $\mathbb{Z}$ and its map $\mathbb{Z}[\mu](t)$ as

$$\begin{cases} \mathbb{Z} : \mathcal{A}(\mathbb{I}) \to \mathcal{B}(\mathbb{I}), \\ \mathbb{Z}[\mu](t) = {}_0^{ABC}\partial_t^{\delta}\mu(t). \end{cases} \tag{10}$$

Based on this, if $\zeta(t, \mu(t), \partial_t\mu(t)) := \bar{\gamma}(t) - \bar{\eta}(\mu(t)) - \bar{\lambda}(\mu(t))\,\partial_t\mu(t)$, then Eq. (9) can be converted into the form of

$$\begin{cases} \mathbb{Z}[\mu](t) = \zeta(t, \mu(t), \partial_t\mu(t)), \\ \mu(0) = 0, \\ \partial_t\mu(0) = 0. \end{cases} \tag{11}$$

Following, we will organize and construct system of orthogonal functions using the subsequent steps: put $\mathcal{S}_i(t) = \mathcal{N}_{t_i}(t)$ and $\Lambda_i(t) = \mathbb{Z}^*[\mathcal{S}_i](t)$, $i = 1, 2, 3, \ldots$, where $\mathbb{Z}^*$ is the adjoint operator of $\mathbb{Z}$, and $\{t_i\}_{i=1}^{\infty}$ is dense on $\mathbb{I}$.

Generally, the Gram–Schmidt orthogonalization process used to generate the systems of orthonormal functions $\{\bar{\Lambda}_i(t)\}_{i=1}^{\infty}$ on $\mathcal{A}(\mathbb{I})$. Aught, if one refer to the orthogonalization coefficients by ε_{ik} in the indexes $i = 2, 3, \ldots$, and $k = 1, 2, \ldots i-1$, then

$$\bar{\Lambda}_i(t) = \sum_{k=1}^{i} \omega_{ik}\Lambda_k(t). \tag{12}$$

At all event, if $\langle \mu(t), \Lambda_i(t)\rangle_{\mathcal{A}} = 0$, $i = 1, 2, \ldots$, then $\langle \mu(t), \Lambda_i(t)\rangle_{\mathcal{A}} = \langle \mu(t), \mathbb{Z}^*[\mathcal{S}_i](t)\rangle_{\mathcal{A}} = \langle \mathbb{Z}[\mu](t), \mathcal{S}_i(t)\rangle_{\mathcal{B}} = \mathbb{Z}[\mu](t_i) = 0$ Calling up that, $\mu(t) = \langle \mu(\cdot), \mathbb{M}_t(\cdot)\rangle_{\mathcal{A}}$, this award $\mathbb{Z}[\mu](t) = \langle \mathbb{Z}[\mu](t), \mathcal{S}_i(t)\rangle_{\mathcal{A}} = 0$. By the density of $\{t_i\}_{i=1}^{\infty}$ on $\mathbb{A}$, we have got $\mathbb{Z}[\mu](t) = 0$. During the existence of $\mathbb{Z}^{-1}$, yields $\mu(t) = 0$. Subsequently, $\{\Lambda_i(t)\}_{i=1}^{\infty}$ is a complete on $\mathcal{A}(\mathbb{I})$. One more, $\Lambda_i(t) = \mathbb{Z}^*[\mathcal{S}_i](t) = \langle \mathbb{Z}^*[\mathcal{S}_i](s), \mathcal{M}_t(s)\rangle_{\mathcal{A}} = \langle \mathcal{S}_i(s), \mathbb{O}_s[\mathcal{M}_t](s)\rangle_{\mathcal{B}} = \mathbb{Z}_s[\mathcal{M}_t](s)|_{s=t_i}$. Visibly, this will generate the subordinate result; the system $\{\Lambda_i(t)\}_{i=1}^{\infty}$ is complete and $\Lambda_i(t) = \mathbb{Z}_s[\mathcal{M}_t](s)|_{s=t_i}$.

Theorem 3. *Assume that ε_{ik} are orthogonalization coefficients for the orthonormal functions systems $\{\bar{\Lambda}_i(t)\}_{i=1}^{\infty}$. Then, the subsequent are achieved:*

(1) *Whenever $n \to \infty$ the analytic solution of Eq. (11) fulfills well*

$$\mu(t) = \sum_{i=1}^{\infty}\sum_{k=1}^{i} \varepsilon_{ik}\zeta\,(t_k, \mu(t_k), \partial_t\mu(t_k))\,\bar{\Lambda}_i(t). \tag{13}$$

(2) *The n-term numerical solution of Eq. (11) fulfills well*

$$\mu^n(t) = \sum_{i=1}^{n}\sum_{k=1}^{i} \varepsilon_{ik}\zeta\,(t_k, \mu(t_k), \partial_t\mu(t_k))\,\bar{\Lambda}_i(t). \tag{14}$$

Proof. The convergent in the emotion of $\|\cdot\|_{\mathcal{A}}$ will gives

$$\begin{aligned} \mu(t) &= \sum_{i=1}^{\infty} \langle \mu(t), \bar{\Lambda}_i(t)\rangle_{\mathcal{W}}\,\bar{\Lambda}_i(t) \\ &= \sum_{i=1}^{\infty} \left\langle \mu(t), \sum_{k=1}^{i} \varepsilon_{ik}\Lambda_k(t) \right\rangle_{\mathcal{A}} \bar{\Lambda}_i(t) \\ &= \sum_{i=1}^{\infty}\sum_{k=1}^{i} \varepsilon_{ik}\langle \mu(t), \mathbb{Z}^*[\mathcal{S}_k](t)\rangle_{\mathcal{A}}\,\bar{\Lambda}_i(t) \\ &= \sum_{i=1}^{\infty}\sum_{k=1}^{i} \varepsilon_{ik}\langle \mathbb{Z}[\mu](t), \mathcal{S}_k(t)\rangle_{\mathcal{B}}\,\bar{\Lambda}_i(t) \end{aligned}$$

$$= \sum_{i=1}^{\infty}\sum_{k=1}^{i}\varepsilon_{ik}\left\langle \zeta\left(t,\mu\left(t\right),\partial_t\mu\left(t\right)\right),\mathcal{S}_k\left(t\right)\right\rangle_{\mathcal{B}}\bar{\Lambda}_i\left(t\right)$$

$$= \sum_{i=1}^{\infty}\sum_{k=1}^{i}\varepsilon_{ik}\zeta\left(t_k,\mu\left(t_k\right),\partial_t\mu\left(t_k\right)\right)\bar{\Lambda}_i\left(t\right). \quad (15)$$

This due to the fact that $\left\langle \mu\left(t\right),\mathcal{S}_i\left(t\right)\right\rangle_{\mathcal{A}} = \mu\left(t_i\right)$ and $\sum_{i=1}^{\infty}\left\langle \mu\left(t\right),\bar{\Lambda}_i\left(t\right)\right\rangle_{\mathcal{A}}\bar{\Lambda}_i\left(t\right)$ is the Fourier series amplification around $\left\{\bar{\Lambda}_i\left(t\right)\right\}_{i=1}^{\infty}$. Ultimately, for numerical computations, we truncated the series in Eq. (13) and creating the n-term numerical solution of $\mu\left(t\right)$. □

4. CONVERGENCE AND ERROR CONDUCTANCE

This section is devoted to describe the convergence of the FRKM for solving FLE in the ABC sense beneath the compatibility conditions of the existence, uniqueness, and adequate differentiability in the Hilbert domain $\mathcal{A}\left(\mathbb{I}\right)$. To achieve our goal, we undertake $\left\|\mu^{n-1}\right\|_{\mathcal{A}}$ is bounded whenever $n \to \infty$ and $\{t_i\}_{i=1}^{\infty}$ is dense on $\mathbb{I}$.

To ensure that the error will decrease for sufficiently large n, it is apparent that

$$\begin{aligned}\left\|\mu-\mu^n\right\|_{\mathcal{A}}^2 &= \left\|\sum_{i=n+1}^{\infty}\left\langle \mu\left(t\right),\bar{\Lambda}_i\left(t\right)\right\rangle_{\mathcal{A}}\bar{\Lambda}_i\left(t\right)\right\|_{\mathcal{A}}^2\\ &= \sum_{i=n+1}^{\infty}\left\langle \mu\left(t\right),\bar{\Lambda}_i\left(t\right)\right\rangle_{\mathcal{A}}^2\\ &\le \sum_{i=n}^{\infty}\left\langle \mu\left(t\right),\bar{\Lambda}_i\left(t\right)\right\rangle_{\mathcal{A}}^2\\ &= \left\|\sum_{i=n}^{\infty}\left\langle \mu\left(t\right),\bar{\Lambda}_i\left(t\right)\right\rangle_{\mathcal{A}}\bar{\Lambda}_i\left(t\right)\right\|_{\mathcal{A}}^2\\ &= \left\|\mu-\mu^{n-1}\right\|_{\mathcal{A}}^2. \end{aligned} \quad (16)$$

Consequently, $\{\|\mu-\mu^n\|_{\mathcal{A}}\}_{n=1}^{\infty}$ is decreasing in $\|\bullet\|_{\mathcal{A}}$. Using the convergent fact on $\sum_{i=1}^{\infty}\langle\mu\left(t\right), \bar{\Lambda}_i\left(t\right)\rangle_{\mathcal{A}}\bar{\Lambda}_i\left(t\right)$ yields that $\|\mu-\mu^n\|_{\mathcal{A}}^2 \to 0$ whenever $n \to \infty$ as long as $\mu\left(t\right)$ and $\mu^n\left(t\right)$ are extracted from Eqs. (13) and (14), respectively. Visibly, this will generate the subordinate result; the sequence of error $\{\|\mu-\mu^n\|_{\mathcal{A}}\}_{n=1}^{\infty}$ is decreasing in $\mathcal{A}\left(\mathbb{I}\right)$ and $\|\mu-\mu^n\| \to 0$ whenever $n \to \infty$.

Lemma 1. *Whenever* $\mu \in \mathcal{A}\left(\mathbb{I}\right)$, *thereafter* $\left|\mu\left(t\right)\right| \le 3.5\left\|\mu\right\|_{\mathcal{A}}$, $\left|\partial_t\mu\left(t\right)\right| \le 3\left\|\mu\right\|_{\mathcal{A}}$, *and* $\left|\partial_t^2\mu\left(t\right)\right| \le 2\left\|\mu\right\|_{\mathcal{A}}$.

Proof. Hither, we will consider $\left|\mu\left(t\right)\right|$ exclusively. The perception that $\partial_t^2\mu\left(t\right) - \partial_t^2\mu\left(0\right) = \int_0^t\partial_p^3\mu\left(p\right)dp$ and integrated it from to t, the result is

$$\partial_t\mu\left(t\right) - \partial_t\mu\left(0\right) - \partial_t^2\mu\left(0\right)t = \int_0^t\int_0^u\partial_p^3\mu\left(p\right)dp\,du. \quad (17)$$

Integrating again from to t yields that

$$\mu\left(t\right) - \mu\left(0\right) - \partial_t\mu\left(0\right)t - 0.5\partial_t^2\mu\left(0\right)t^2 = \int_0^t\int_0^v\int_0^u\partial_p^3\mu\left(p\right)dp\,du\,dv. \quad (18)$$

Taking the usual metric functions length yields that

$$\left|\mu\left(t\right)\right| \le \left|\mu\left(0\right)\right| + \left|\partial_t\mu\left(0\right)\right|\left|t\right| + \frac{1}{2}\left|\partial_t^2\mu\left(0\right)\right|\left|t\right|^2 + \int_{\mathbb{I}}\left|\partial_p^3\mu\left(p\right)\right|dp. \quad (19)$$

After rearranging the mathematical formulation, one finds

$$\left|\mu\left(t\right)\right| \le \left|\mu\left(0\right)\right| + \left|\partial_t\mu\left(0\right)\right| + 0.5\left|\partial_t^2\mu\left(0\right)\right| + \int_{\mathbb{I}}\left|\partial_p^3\mu\left(p\right)\right|dp. \quad (20)$$

Using Holder's inequality and Eq. (5), we can note the dependency

$$\begin{aligned}\left|\partial_p^k\mu\left(0\right)\right|_{k=0,1,2} &\le \left(\left(\mu\left(0\right)\right)^2 + \left(\partial_t\mu\left(0\right)\right)^2 + \left(\partial_t^2\mu\left(0\right)\right)^2 + \int_{\mathbb{I}}\left(\partial_p^3\mu\left(p\right)\right)^2dt\right)^{\frac{1}{2}}\\ &= \left\|u\right\|_{\mathcal{A}}, \end{aligned} \quad (21)$$

$$\begin{aligned}\int_{\mathbb{I}}\left|\partial_p^3\mu\left(p\right)\right|dp &\le \left(\int_{\mathbb{I}}\left(\partial_p^3\mu\left(p\right)\right)^2dp\int_{\mathbb{I}}\left(1\right)^2dp\right)^{\frac{1}{2}}\\ &\le \left(\left(\mu\left(0\right)\right)^2 + \left(\partial_t\mu\left(0\right)\right)^2 + \left(\partial_t^2\mu\left(0\right)\right)^2 + \int_{\mathbb{I}}\left(\partial_p^3\mu\left(p\right)\right)^2dt\right)^{\frac{1}{2}}\\ &= \left\|u\right\|_{\mathcal{A}}. \end{aligned} \quad (22)$$

Thus, by amalgamating the overhead results one get $\left|\mu\left(t\right)\right| \le 3.5\left\|\mu\right\|_{\mathcal{A}}$. □

Theorem 4. *Let* $\zeta(t,\mu(t),\partial_t\mu(t)) \in \mathcal{C}(\mathbb{A}\times\mathbb{R}\times\mathbb{R},\mathbb{R})$. *If* $\left\|\mu^{n-1}-\mu\right\|_{\mathcal{A}} \to 0, t_n \to s$ *whenever* $n\to\infty$, *then as* $n\to\infty$

$$\zeta\left(t_n,\mu^{n-1}(t_n),\partial_t\mu^{n-1}(t_n)\right) \to \zeta(s,\mu(s),\partial_t\mu(s)). \quad (23)$$

Proof. First, we will prove that $\partial_t^k\mu^{n-1}(t_n) \to \partial_t^k\mu(s)$, $k=0,1$. Since, we can note that

$$\begin{aligned}&\left|\partial_t^k\mu^{n-1}(t_n)-\partial_t^k\mu(s)\right|\\ &=\left|\partial_t^k\mu^{n-1}(t_n)-\partial_t^k\mu^{n-1}(s)\right.\\ &\quad\left.+\partial_t^k\mu^{n-1}(s)-\partial_t^k\mu(s)\right|\\ &\le\left|\partial_t^k\mu^{n-1}(t_n)-\partial_t^k\mu^{n-1}(s)\right|\\ &\quad+\left|\partial_t^k\mu^{n-1}(s)-\partial_t^k\mu(s)\right|\\ &\le\left|\partial_t^{k+1}\mu^{n-1}(\xi)\right||t_n-s|\\ &\quad+\left|\partial_t^k\mu^{n-1}(s)-\partial_t^k\mu(s)\right|\\ &\le\mathbb{O}_1\left\|\mu^{n-1}\right\|_{\mathcal{A}}|t_n-s|+\mathbb{O}_2\left\|\mu^{n-1}-\mu\right\|_{\mathcal{A}}, \quad (24)\end{aligned}$$

where ξ in between $(\min\{t_n,s\},\max\{t_n,s\})$ and

$$(\mathbb{O}_1,\mathbb{O}_2)=\begin{cases}(3,3.5), & k=0,\\ (2,3), & k=1.\end{cases}$$

It pursues that $\left|\mu^{n-1}(t_n)-\mu(s)\right| \to 0$ whenever $n\to\infty$. By means of $\zeta(t,\mu(t),\partial_t\mu(t)) \in \mathcal{C}(\mathbb{A}\times\mathbb{R}\times\mathbb{R},\mathbb{R})$ it implies the demanded. □

Thereafter, we will symbolize $\mathcal{F}_i = \sum_{k=1}^{i}\varepsilon_{ik}\zeta(t_k,\mu(t_k),\partial_t\mu(t_k))$. In fact, this allows one to put $\mu^n(t)$ as

$$\mu^n(t)=\sum_{i=1}^{n}\mathcal{F}_i\bar{\Lambda}_i(t). \quad (25)$$

Theorem 5. *In the iterative formula of Eq.* (25), *one has* $\mu^n(t)\to\mu(t)$ *whenever* $n\to\infty$.

Proof. From Eq. (25), we deduce that $\mu^{n+1}(t) = \mu^n(t) + \mathcal{F}_{n+1}\bar{\Lambda}_{n+1}(t)$. From orthogonality of $\left\{\bar{\Lambda}_i(t)\right\}_{i=1}^{\infty}$ one acquired

$$\begin{aligned}\left\|\mu^{n+1}\right\|_{\mathcal{A}}^2&=\left\|\mu^{n}\right\|_{\mathcal{A}}^2+\mathcal{F}_{n+1}^2\\ &=\left\|\mu^{n-1}\right\|_{\mathcal{A}}^2+\mathcal{F}_{n}^2+\mathcal{F}_{n+1}^2\\ &=\cdots\\ &=\left\|\mu^{0}\right\|_{\mathcal{A}}^2+\sum_{i=1}^{n+1}\mathcal{F}_i^2. \quad (26)\end{aligned}$$

This gives $\left\|\mu^{n+1}\right\|_{\mathcal{A}} \ge \left\|\mu^{n}\right\|_{\mathcal{A}}$ and $\exists\gamma\in\mathbb{R}$ such that $\sum_{i=1}^{\infty}\mathcal{F}_i^2=\gamma$, which glimpse that $\left\{\mathcal{F}_i^2\right\}_{i=1}^{\infty}\in l^2$. In order to

$$\begin{aligned}&\mu^m(t)-\mu^{m-1}(t)\perp\mu^{m-1}(t)-\mu^{m-2}(t)\\ &\quad\perp\cdots\perp\mu^{n+1}(t)-\mu^n(t), \quad (27)\end{aligned}$$

it succeed for $m>n$ that

$$\begin{aligned}&\left\|\mu^m-\mu^n\right\|_{\mathcal{A}}^2\\ &\quad=\left\|\mu^m-\mu^{m-1}+\mu^{m-1}-\cdots+\mu^{n+1}-\mu^n\right\|_{\mathcal{A}}^2\\ &\quad=\left\|\mu^m-\mu^{m-1}\right\|_{\mathcal{A}}^2+\left\|\mu^{m-1}-\mu^{m-2}\right\|_{\mathcal{A}}^2\\ &\qquad+\cdots+\left\|\mu^{n+1}-\mu^n\right\|_{\mathcal{A}}^2, \quad (28)\end{aligned}$$

whereas $\left\|\mu^m-\mu^{m-1}\right\|_{\mathcal{A}}^2=\mathcal{F}_m^2$. So, whenever $nm\to\infty$, one has $\left\|\mu^m-\mu^n\right\|_{\mathcal{A}}^2=\sum_{l=n+1}^{m}\mathcal{F}_i^2\to 0$ and by the completeness $\exists\mu^n(t)\in\mathcal{A}(\mathbb{I})$ such that $\mu^n(t)\to\mu(t)$ as $n\to\infty$ in the emotion of $\|\bullet\|_{\mathcal{A}}$. □

Theorem 6. *In the iterative formula of Eq.* (25), *one has* $\mu(t)=\sum_{i=1}^{\infty}\mathcal{F}_i\bar{\Lambda}_i(t)$ *whenever* $n\to\infty$.

Proof. But in return, by taking $(\bullet)$ on both sides of Eq. (25), one get $\mu(t)=\sum_{i=1}^{\infty}\mathcal{F}_i\bar{\Lambda}_i(t)$, while $\mathbb{Z}[\mu](t)=\sum_{i=1}^{\infty}\mathcal{F}_i\mathbb{Z}\left[\bar{\Lambda}_i\right](t)$, thus

$$\begin{aligned}\mathbb{Z}[\mu](t_l)&=\sum_{i=1}^{\infty}\mathcal{F}_i\left\langle\mathbb{Z}\left[\bar{\Lambda}_i\right](t),\mathcal{S}_l(t)\right\rangle_{\mathcal{B}}\\ &=\sum_{i=1}^{\infty}\mathcal{F}_i\left\langle\bar{\Lambda}_i(t),\mathbb{Z}^*\left[\mathcal{S}_l\right](t)\right\rangle_{\mathcal{A}}\\ &=\sum_{i=1}^{\infty}\mathcal{F}_i\left\langle\bar{\Lambda}_i(t),\Lambda_l(t)\right\rangle_{\mathcal{A}}, \quad (29)\end{aligned}$$

$$\begin{aligned}\sum_{l'=1}^{l}\varepsilon_{ll'}\mathbb{Z}[\mu](t_{l'})&=\sum_{i=1}^{\infty}\mathcal{F}_i\left\langle\bar{\Lambda}_i(t),\sum_{l'=1}^{l}\varepsilon_{ll'}\Lambda_{l'}(t)\right\rangle_{\mathcal{A}}\\ &=\sum_{i=1}^{\infty}\mathcal{F}_i\left\langle\bar{\Lambda}_i(t),\bar{\Lambda}_{l'}(t)\right\rangle_{\mathcal{A}}\\ &=\mathcal{F}_l. \quad (30)\end{aligned}$$

Justificatory, if $l=1$, then $\mathbb{Z}[\mu](t_1)=\zeta\left(t_1,\mu^0(t_1),\partial_t\mu^0(t_1)\right)$. Still, if $l=2$, then $\mathbb{Z}[\mu](t_2)=\zeta\left(t_2,\mu^1(t_2),\partial_t\mu^1(t_2)\right)$. In analogous route, the modality form is $\mathbb{Z}[\mu](t_n)=\zeta\left(t_n,\mu^{n-1}(t_n),\partial_t\right.$

$\mu^{n-1}(t_n)\big)$. By the density condition, $\forall s \in \mathbb{I}$; $\exists \left\{t_{n_q}\right\}_{q=1}^{\infty}$ such that $t_{n_q} \to s$ whenever $q \to \infty$ or $\mathbb{Z}[\mu]\left(t_{n_q}\right) = \zeta\left(t_{n_q}, \mu^{n_q-1}\left(t_{n_q}\right), \partial_t \mu^{n_q-1}\left(t_{n_q}\right)\right)$. Let $j \to \infty$ one get $\mathbb{Z}[\mu](s) = \zeta(s, \mu(s), \partial_t \mu(s))$. Also, since $\bar{\Lambda}_i(t) \in \mathcal{A}(\mathbb{I})$, then $\mu(t)$ satisfies Eq. (11). Eventually, the uniqueness of solution on Eq. (11) utilizes the required score. □

5. NUMERICAL APPLICATIONS AND COMPUTATIONAL RESULTS

This section utilizes some numerical applications with different fractional order parameters for model of FLE in the ABC fractional sense. The numerical results are discussed graphically and quantitatively to verify the validity and applicability of the proposed FRKM in obtaining accurate numerical solutions for those models. Mathematica 10 software package is used in all computational process.

5.1. The FRKM Steps

The attached steps focusing on the computational steps required using an appropriate software package for solving Eq. (11) using FRKM. In this Procedure and Algorithm, some subsequent inputs are needed so as to deduce the numerical reckoning μ^n of μ in $\mathcal{A}(\mathbb{I})$.

Procedure 1. Steps of the orthonormal Gram–Schmidt process:

Step 1: For $i = 2, 3, \ldots$, and $k = 1, 2, \ldots i-1$, do the following:

$$\varepsilon_{ik} = \begin{cases} \dfrac{1}{\|\Lambda_1\|_{\mathcal{A}}}, i = k = 1, \\ \dfrac{1}{\sqrt{\|\Lambda_i\|_{\mathcal{A}}^2 - \sum_{p=1}^{i-1} \langle \Lambda_i(t), \bar{\Lambda}_p(t) \rangle_{\mathcal{A}}^2}}, \\ \qquad i = k \neq 1, \\ -\dfrac{1}{\sqrt{\|\Lambda_i\|_{\mathcal{A}}^2 - \sum_{p=1}^{i-1} \langle \Lambda_i(t), \bar{\Lambda}_p(t) \rangle_{\mathcal{A}}^2}} \\ \quad \displaystyle\sum_{p=k}^{i-1} \langle \Lambda_i(t), \bar{\Lambda}_p(t) \rangle_{\mathcal{A}} \omega_{pk}, i > k. \end{cases} \tag{31}$$

Output: The orthogonalization coefficients ε_{ik}.

Step 2: For $i = 1, 2, 3, \ldots$ set

$$\bar{\Lambda}_i(t) = \sum_{k=1}^{i} \varepsilon_{ik} \Lambda_k(t). \tag{32}$$

Output: systems of orthonormal functions $\left\{\bar{\Lambda}_i(t)\right\}_{i=1}^{\infty}$.

Algorithm 1. Steps of FRKM for numerical reckonings model of FLE in ABC approach.

Step I: Fixed t, s in $\mathbb{I}$ and do Phases 1 and 2:
- **Phase 1:** Set $t_i = \frac{1}{n} i$ in the indices $i = 0, 1, \ldots, n$.
- **Phase 2:** Set $\Lambda_i(t) = \mathbb{Z}[\mathcal{M}_t](s)|_{s=t_i}$ in the indices $i = 1, 2, \ldots, n$.

Output: The orthogonal function system $\Lambda_i(t)$.
Step II: In the indices $i = 1, 2, \ldots$ and $k = 1, 2, \ldots, i-1$ do Procedure 1..
Output: The orthogonalization coefficients ε_{ik}.
Step III: Set $\bar{\Lambda}_i(t) = \sum_{k=1}^{i} \varepsilon_{ik} \Lambda_k(t)$ in the indices $i = 1, 2, \ldots, n$.
Output: The orthonormal function system $\bar{\Lambda}_i(t)$.
Step IV: Set $\mu^0(t_1) = 0$ and in the index $i = 1, 2, \ldots, n$ do Phases 1–3:
- **Phase 1:** Set $\mu^i(t_i) = \mu^{i-1}(t_i)$.
- **Phase 2:** Set $\mathcal{F}_i = \sum_{k=1}^{i} \varepsilon_{ik} \zeta(t_k, \mu(t_k), \partial_t \mu(t_k))$.
- **Phase 3:** Set $\mu^n(t) = \sum_{k=1}^{i} \mathcal{F}_k \bar{\Lambda}_k(t)$.

Output: The n-term numerical reckoning $\mu^n(t)$ of $\mu(t)$.

5.2. Test Applications

To fill our present results in the form of realistic and tangible models, three applications for model of FLE in the ABC fractional sense containing forcing term in its nonhomogeneous part are discussed. The readers should be noted thither that in the next three applications $\mu(0)$ and $\partial_t \mu(0)$ are known and may not homogeneous.

Application 1. Essentially, let allow us behold the subsequent model of FLE in ABC approach:

$$\begin{cases} {}_0^{ABC}\partial_t^{\delta} \mu(t) + 3\mu(t) - 2\mu^3(t) = \gamma(t), \\ \mu(0) = 0, \\ \partial_t \mu(0) = 1. \end{cases} \tag{33}$$

with forcing term $\gamma(t) = \cos(t) \sin(2t)$ and the exact solution when $\delta = 2$ agree well with

$$\mu(t) = \sin(t). \tag{34}$$

Application 2. Now, let allow us behold the subsequent model of FLE in ABC approach:

$$\begin{cases} {}_0^{ABC}\partial_t^{\delta} \mu(t) + \mu(t) \partial_t \mu(t) - 6e^{\mu(t)} = \gamma(t), \\ \mu(0) = 0, \\ \partial_t \mu(0) = 0 \end{cases} \tag{35}$$

with forcing term $\gamma(t) = 6t - 6e^{t^3} + 3t^5$ and the exact solution when $\delta = 2$ agree well with

$$\mu(t) = t^3. \tag{36}$$

Application 3. Finally, let allow us behold the subsequent model of FLE in ABC approach:

$$\begin{cases} {}_0^{ABC}\partial_t^{\delta} \mu(t) + \left(\mu^2(t) + 1\right) \partial_t \mu(t) - \mu(t) \\ \quad - \cosh(t) \mu^2(t) = \gamma(t), \\ \mu(0) = 0, \\ \partial_t \mu(0) = 1. \end{cases}$$

with forcing term $\gamma(t) = \cosh(t)$ and the exact solution when $\delta = 2$ agree well with

$$\mu(t) = \sinh(t). \tag{37}$$

In those three applications, the researchers should note that the absence of analytic solutions does not have much effect on the gained results, because we will obtain and plot the numerical solutions at different values of δ.

5.3. Results and Discussions

Occupancy $t_i = i/n$ in the indices $i = 0, 1, \ldots, n = 50$ on $\mathbb{I}$ in $\mu^n(t_i)$ and then applying Procedure 1. and Algorithm 1.. Anyhow, we apply the FRKM to discuss the previous three applications in which $t \in \mathbb{I}$, $\delta \in [1, 2] - \{1\}$.

Following, numerical validations for different values of grid points $t_i \in \mathbb{I}$ when $\delta = 2$ will be exhibited. For this purpose, Tables 1–3 tabulate the evolution of exact solutions $\mu(t_i)$, numerical solutions $\mu^{21}(t_i)$, absolute errors $\mathcal{Ab}[\mu^{50}](t_i)$, and relative errors $\mathfrak{Re}[\mu^{50}](t_i)$ for Applications 1–3, respectively, where

$$\mathcal{Ab}[\mu^{50}](t_i) = \left|\mu(t_i) - \mu^{50}(t_i)\right|, \tag{38}$$

$$\mathfrak{Re}[\mu^{50}](t_i) = \left|\mu(t_i) - \mu^{50}(t_i)\right| |\mu(t_i)|^{-1}. \tag{39}$$

Our next analysis is to explicate numerical solutions $\mu^n(t_i)$ of the FRKM in solving model of FLE in ABC approach. For this purpose, the contract between the numerical solutions when $\delta \in \{2, 1.9, 1.8, 1.7\}$ is investigated in Tables 4–6 for Applications 1–3, respectively, at various $t_i \in \mathbb{I}$. It is obvious from the tables that there are good harmony and agreement between the presented data whether for $\delta = 2$ or $\delta \in \{1.9, 1.8, 1.7\}$.

Of the data gained, it can be observed that the columns tables almost match, similar in their digits, and in good agreement with each other, especially when considering the integer-order derivative. Indeed, the ABC fractional orders have

Table 1 **Numerical Results of Application 1 When $\delta = 2$ Using Algorithm 1..**

t_i	$\mu(t_i)$	$\mu^{50}(t_i)$	$\mathcal{Ab}[\mu^{50}](t_i)$	$\mathfrak{Re}[\mu^{50}](t_i)$
0	0	0	0	Indeterminate
0.1	0.099833417	0.099833416	$3.789779185 \times 10^{-10}$	$3.796102860 \times 10^{-9}$
0.2	0.198669331	0.198669331	$2.666233068 \times 10^{-10}$	$1.342045628 \times 10^{-9}$
0.3	0.295520207	0.295520207	$1.124974558 \times 10^{-10}$	$3.806760190 \times 10^{-10}$
0.4	0.389418342	0.389418342	$6.275274744 \times 10^{-11}$	$1.611448168 \times 10^{-10}$
0.5	0.479425539	0.479425539	$2.430054491 \times 10^{-10}$	$5.068679691 \times 10^{-10}$
0.6	0.564642473	0.564642474	$4.111170293 \times 10^{-10}$	$7.281014955 \times 10^{-10}$
0.7	0.644217687	0.644217688	$5.580612639 \times 10^{-10}$	$8.662619405 \times 10^{-10}$
0.8	0.717356091	0.717356092	$6.050903112 \times 10^{-10}$	$8.435006252 \times 10^{-10}$
0.9	0.783326910	0.783326912	$2.675715094 \times 10^{-9}$	$3.415834514 \times 10^{-9}$
1.0	0.841470985	0.841470994	$9.160235348 \times 10^{-9}$	$1.088597886 \times 10^{-8}$

Table 2 **Numerical Results of Application 2 When $\delta = 2$ Using Algorithm 1..**

t_i	$\mu(t_i)$	$\mu^{50}(t_i)$	$\mathcal{Ab}[\mu^{50}](t_i)$	$\mathfrak{Re}[\mu^{50}](t_i)$
0	0	0	0	Indeterminate
0.1	0.001000000	0.000999992	$8.403186007 \times 10^{-9}$	$8.403186007 \times 10^{-6}$
0.2	0.008000000	0.008000002	$1.677179007 \times 10^{-9}$	$2.096473758 \times 10^{-7}$
0.3	0.027000000	0.027000032	$3.230583386 \times 10^{-8}$	$1.196512365 \times 10^{-6}$
0.4	0.064000000	0.064000092	$9.231110808 \times 10^{-8}$	$1.442361064 \times 10^{-6}$
0.5	0.125000000	0.125000191	$1.911998641 \times 10^{-7}$	$1.529598913 \times 10^{-6}$
0.6	0.216000000	0.216000336	$3.356905938 \times 10^{-7}$	$1.554123120 \times 10^{-6}$
0.7	0.343000000	0.343000862	$8.619610321 \times 10^{-7}$	$2.513005924 \times 10^{-6}$
0.8	0.512000000	0.512001151	$1.151361527 \times 10^{-6}$	$2.248752982 \times 10^{-6}$
0.9	0.729000000	0.729000937	$9.367440478 \times 10^{-7}$	$1.284971259 \times 10^{-6}$
1.0	1.000000000	1.000000510	$5.095803186 \times 10^{-7}$	$5.095803186 \times 10^{-7}$

Table 3 Numerical Results of Application 3 When $\delta = 2$ Using Algorithm 1..

t_i	$\mu(t_i)$	$\mu^{50}(t_i)$	$\mathcal{Ab}[\mu^{50}](t_i)$	$\mathfrak{Re}[\mu^{50}](t_i)$
0	0	0	0	Indeterminate
0.1	0.100166750	0.100166967	$2.172963557 \times 10^{-7}$	$2.169346172 \times 10{-}6$
0.2	0.201336003	0.201336261	$2.589315430 \times 10^{-7}$	$1.286066773 \times 10{-}6$
0.3	0.304520293	0.304520543	$2.497367032 \times 10^{-7}$	$8.200987211 \times 10{-}7$
0.4	0.410752326	0.410752588	$2.621567295 \times 10^{-7}$	$6.382355329 \times 10{-}7$
0.5	0.521095305	0.521095589	$2.837283594 \times 10^{-7}$	$5.444845816 \times 10{-}7$
0.6	0.636653582	0.636653900	$3.181711627 \times 10^{-7}$	$4.997555526 \times 10{-}7$
0.7	0.758583702	0.758584068	$3.660353389 \times 10^{-7}$	$4.825246549 \times 10{-}7$
0.8	0.888105982	0.888106411	$4.291121671 \times 10^{-7}$	$4.831767556 \times 10{-}7$
0.9	1.026516726	1.026517235	$5.092519777 \times 10^{-7}$	$4.960971068 \times 10{-}7$
1.0	1.175201194	1.175200630	$5.632861930 \times 10^{-7}$	$4.793104330 \times 10{-}7$

Table 4 Numerical Solutions $\mu^n(t_i)$ of Application 1 When $\delta \in \{2, 1.9, 1.8, 1.7\}$ Using Algorithm 1..

t_i	$\delta = 2$	$\delta = 1.9$	$\delta = 1.8$	$\delta = 1.7$
0	0	0	0	0
0.1	0.099833416	0.098681057	0.097727054	0.096960031
0.2	0.198669331	0.196299255	0.194241208	0.192582953
0.3	0.295520207	0.291966516	0.288794809	0.286232594
0.4	0.389418342	0.384744952	0.380467024	0.376926644
0.5	0.479425539	0.473725124	0.468382649	0.463755356
0.6	0.564642474	0.558030132	0.551698889	0.545904986
0.7	0.644217688	0.636823116	0.629605554	0.622676976
0.8	0.717356092	0.709315906	0.701327938	0.693415503
0.9	0.783326912	0.774778513	0.766138961	0.757420285
1.0	0.841470994	0.832548933	0.823377242	0.813981347

Table 5 Numerical Solutions $\mu^n(t_i)$ of Application 2 When $\delta \in \{2, 1.9, 1.8, 1.7\}$ Using Algorithm 1..

t_i	$\delta = 2$	$\delta = 1.9$	$\delta = 1.8$	$\delta = 1.7$
0	0	0	0	0
0.1	0.000999992	0.008491899	0.015847216	0.030213070
0.2	0.008000002	0.023246733	0.038232993	0.067556082
0.3	0.027000032	0.050333296	0.073292799	0.118289727
0.4	0.064000092	0.095736203	0.126992649	0.188331928
0.5	0.125000191	0.165388312	0.205195734	0.283398045
0.6	0.216000336	0.265184687	0.313690745	0.409059002
0.7	0.343000862	0.400990578	0.458207955	0.570773783
0.8	0.512001151	0.578646608	0.644429612	0.773910228
0.9	0.729000937	0.803972434	0.877997233	1.023759477
1.0	1.000000510	1.082769456	1.164516993	1.325546567

strong effects on the model profiles, which tend to lead to unusual behaviors in the event of a significant departure from the integer value of $\delta = 1$.

The 3D surfaces plots of dynamic and geometric behaviors along the memory and heritage characteristics of the FRKM are given next. Following, the geometrical validations of the approximate solutions for different values of grid points $t_i \in \mathbb{I}$ and $\delta \in [1, 2] - \{1\}$ are exhibited as presented in Figs. 1a–1c for Applications 1–3, respectively.

Table 6 **Numerical Solutions $\mu^n(t_i)$ of Application 3 When $\delta \in \{2, 1.9, 1.8, 1.7\}$ Using Algorithm 1..**

t_i	$\delta = 2$	$\delta = 1.9$	$\delta = 1.8$	$\delta = 1.7$
0.1	0.100166967	0.105043660	0.109678954	0.114216844
0.2	0.201336261	0.211327117	0.220870685	0.230262477
0.3	0.304520543	0.319957575	0.334765519	0.349394163
0.4	0.410752588	0.432008552	0.452464838	0.472726189
0.5	0.521095589	0.548554011	0.575043146	0.601322758
0.6	0.636653900	0.670688807	0.703578920	0.736239157
0.7	0.758584068	0.799545061	0.839176310	0.878548396
0.8	0.888106411	0.936306961	0.982983017	1.029361787
0.9	1.026517235	1.082225025	1.136206438	1.189846652
1.0	1.175200630	1.238630381	1.300129112	1.361242713

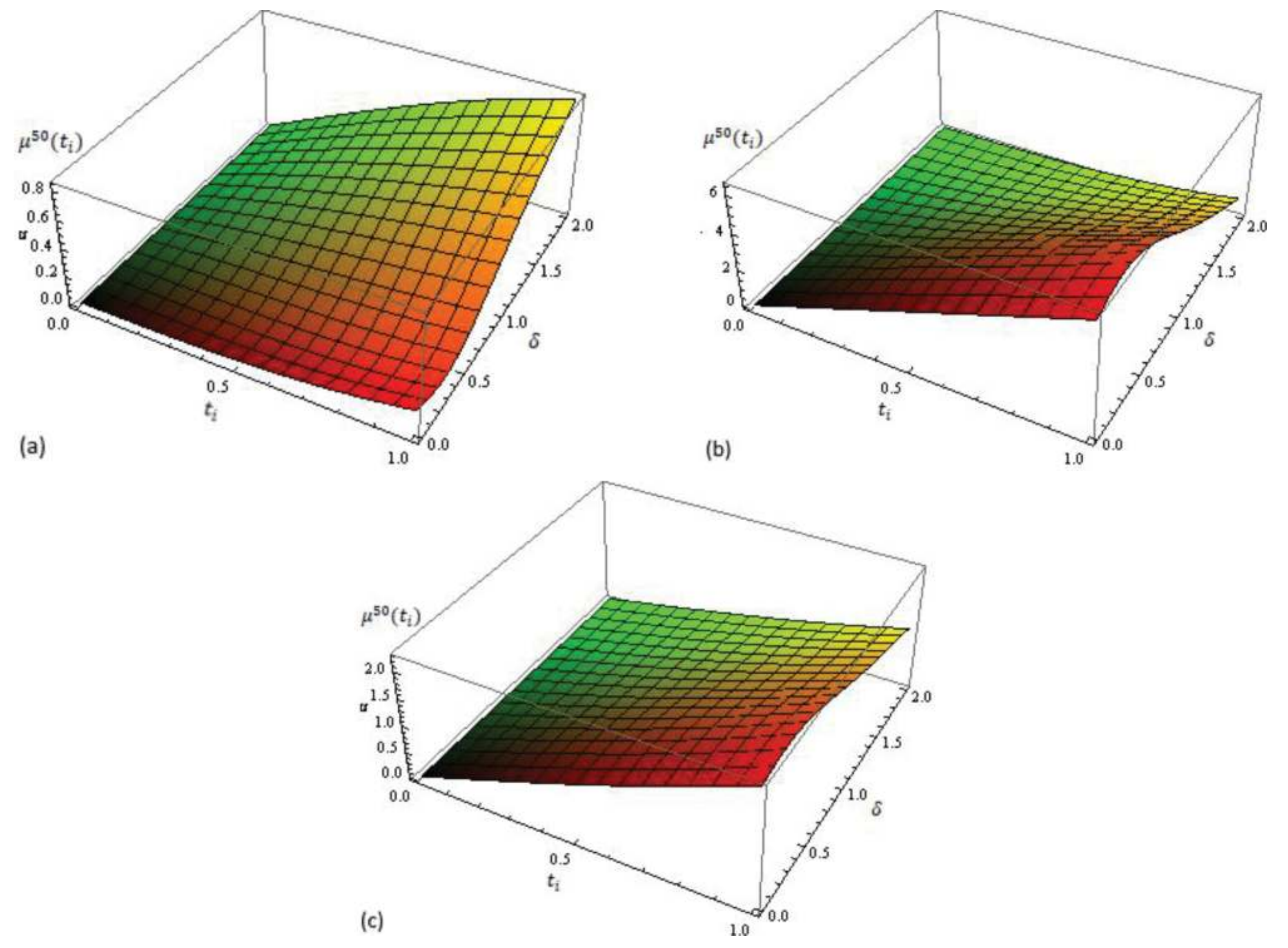

Fig. 1 Comparisons of between the 3D computational values of the FRKM when $t_i \in \mathbb{I}$ and $\delta \in [1, 2] - \{1\}$: (**a**) Application 1, (**b**) Application 2, and (**c**) Application 3.

Finally, as the saying goes, it ended with a refreshing scent; the attitude evaluation of $\mathcal{A}\mathfrak{b}\left[\mu^{50}\right](t_i)$ is examined. Aught, at various $t_i \in \mathbb{I}$ and when $\delta = 2$, Figs. 2a–2c give the 2D relevant plots data of the FRKM elements for Applications 1–3, respectively. It is seen that the expansion in the quantity of hub brings about a decrease in the total errors and correspondingly an improvement in the exactness of the got solutions.

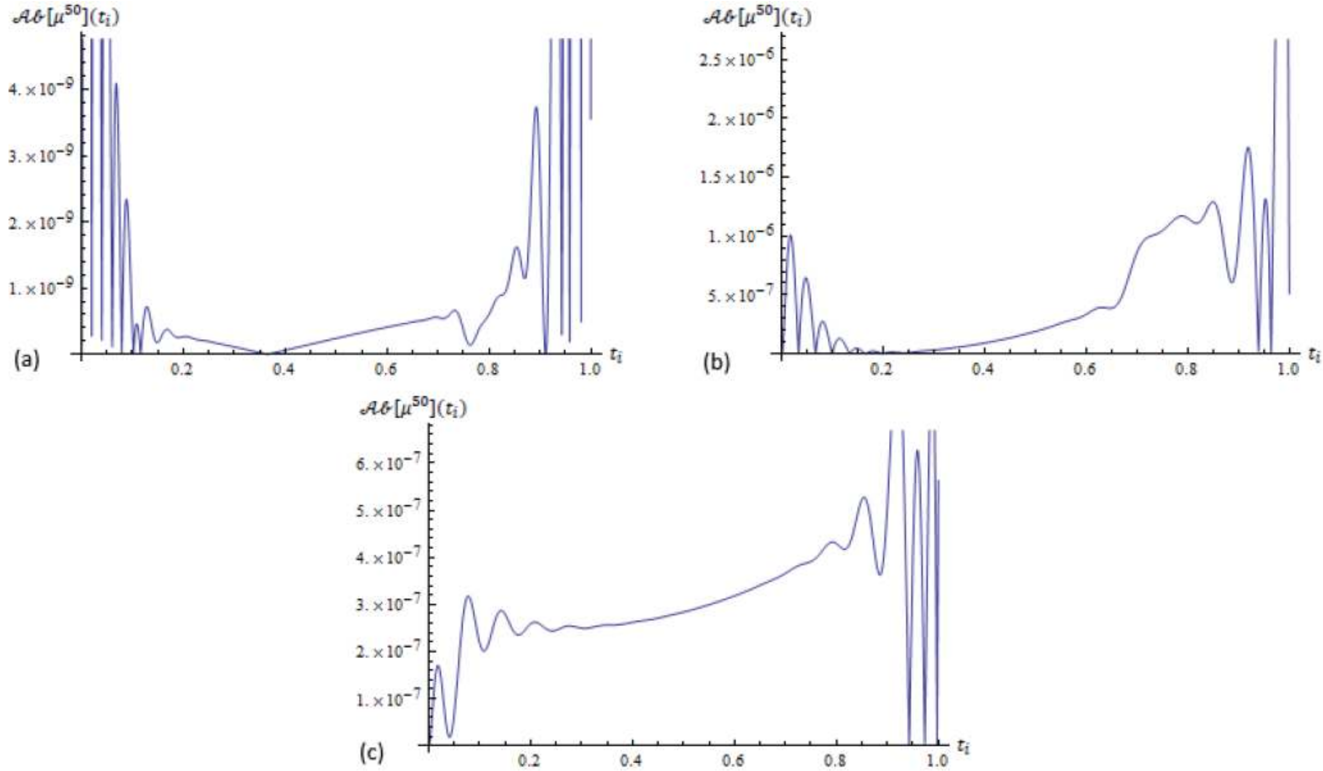

Fig. 2 2D Computational values of $\mathcal{A}\mathfrak{b}\left[\mu^{50}\right](t_i)$ using the FRKM when $t_i \in \mathbb{I}$ and $\delta = 2$: (**a**) Application 1, (**b**) Application 2, and (**c**) Application 3.

6. SUMMARY AND OUTLINE

This article targets to extend the application of the FRKM to explore numerical solutions for model of FLE in the ABC fractional derivative. This target has been successfully achieved using the suggested approach that directly implemented to provide suitable approximations that easily determinable components without any need for transformation or discretization. Some efficacious experiments are presented to validate the capacity and reliability of the approach, where the FRKM results are compared with exact solutions when $\delta = 2$, and with each other for different values of fractional ABC levels, which are found in good agreement with each other even after computing a few iterations. From the numerical and graphical results, it can be concluded that the proposed method is a systematic, powerful, and suitable tool for different nonlinear models, valid for a long time with great potential in scientific applications.

ACKNOWLEDGMENT

This research work is supported by the Ajman University (grant: 2019-20).

REFERENCES

1. R. Herrmann, *Fractional Calculus: An Introduction for Physicists* (World Scientific, Singapore, 2014).
2. V. E. Tarasov, *Fractional Dynamics: Applications of Fractional Calculus to Dynamics of Particles, Fields and Media* (Springer, Germany, 2011).
3. B. J. West, *Fractional Calculus View of Complexity: Tomorrow's Science* (Taylor & Francis, UK, 2015).
4. A. Kilbas, H. Srivastava and J. Trujillo, *Theory and Applications of Fractional Differential Equations* (Elsevier, Netherlands, 2006).
5. B. J. West, *Natures Patterns and the Fractional Calculus* (De Gruyter, Germany, 2017).
6. O. Abu Arqub, Fitted reproducing kernel Hilbert space method for the solutions of some certain classes of time-fractional partial differential equations subject to initial and Neumann boundary conditions, *Comput. Math. Appl.* **73** (2017) 1243–1261.
7. O. Abu Arqub and N. Shawagfeh, Application of reproducing kernel algorithm for solving Dirichlet time-fractional diffusion-Gordon types equations in porous media, *J. Porous Media* **22** (2019) 411–434.
8. O. Abu Arqub, Numerical algorithm for the solutions of fractional order systems of Dirichlet function

types with comparative analysis, *Fundam. Inform.* **166** (2019) 111–137.
9. S. S. Ray, New exact solutions of nonlinear fractional acoustic wave equations in ultrasound, *Comput. Math. Appl.* **71** (2016) 859–868.
10. S. S. Ray and S. Sahoo, Analytical approximate solutions of Riesz fractional diffusion equation and Riesz fractional advection–dispersion equation involving nonlocal space fractional derivatives, *Math. Method. Appl. Sci.* **38** (2015) 2840–2849.
11. M. M. Meerschaert and C. Tadjeran, Finite difference approximations for fractional advection-dispersion flow equations, *J. Comput. Appl. Math.* **172** (2004) 65–77.
12. P. Zhuang, F. Liu, V. Anh and I. Turner, Numerical methods for the variable-order fractional advection–diffusion equation with a nonlinear source term, *SIAM J. Numer. Anal.* **47** (2009) 1760–1781.
13. E. Atilgan, M. Senol, A. Kurt and O. Tasbozan, New wave solutions of time-fractional coupled Boussinesq–Whitham–Broer–Kaup equation as a model of water waves, *China Ocean Eng.* **33** (2019) 477–483.
14. A. Atangana and D. Baleanu, New fractional derivatives with non-local and non-singular kernel: Theory and application to heat transfer model, *Therm. Sci.* **20** (2016) 763–769.
15. A. Atangana and J. J. Nieto, Numerical solution for the model of RLC circuit via the fractional derivative without singular kernel, *Adv. Mech. Eng.* **7** (2015) 1–7.
16. A. Atangana and J. F. Gómez-Aguilar, Decolonisation of fractional calculus rules: Breaking commutativity and associativity to capture more natural phenomena, *Eur. Phys. J. Plus* **133** (2018) 1–22.
17. O. Abu Arqub, Numerical solutions of systems of first-order, two-point BVPs based on the reproducing kernel algorithm, *Calcolo* **55** (2018) 1–28.
18. O. Abu Arqub and B. Maayah, Modulation of reproducing kernel Hilbert space method for numerical solutions of Riccati and Bernoulli equations in the Atangana-Baleanu fractional sense, *Chaos Solitons Fractals* **125** (2019) 163–170.
19. O. Abu Arqub and B. Maayah, Numerical solutions of integrodifferential equations of Fredholm operator type in the sense of the Atangana–Baleanu fractional operator, *Chaos Solitons Fractals* **117** (2018) 117–124.
20. O. Abu Arqub and B. Maayah, Fitted fractional reproducing kernel algorithm for the numerical solutions of ABC-Fractional Volterra integro-differential equations, *Chaos Solitons Fractals* **126** (2019) 394–402.
21. J. D. Djida, A. Atangana and I. Area, Numerical computation of a fractional derivative with non-local and non-singular kernel, *Math. Model. Nat. Phenom.* **12** (2017) 4–13.
22. A. Atangana and J. F. Gómez-Aguilar, Fractional derivatives with no-index law property: Application to chaos and statistics, *Chaos Solitons Fractals* **114** (2018) 516–535.
23. A. Atangana, On the new fractional derivative and application to nonlinear Fisher's reaction–diffusion equation, *Appl. Math. Comput.* **273** (2016) 948–956.
24. A. Atangana and I. Koca, On the new fractional derivative and application to Nonlinear Baggs and Freedman model, *J. Nonlinear. Sci. Appl.* **9** (2016) 2467–2480.
25. O. Algahtani, Comparing the Atangana–Baleanu and Caputo–Fabrizio derivative with fractional order: Allen Cahn model, *Chaos Solitons Fractals* **89** (2016) 552–559.
26. D. Kumara, R. P. Agarwal and J. Singh, A modified numerical scheme and convergence analysis for fractional model of Lienard's equation, *J. Comput. Appl. Math.* **339** (2018) 405–413.
27. D. I. Sinelshchikov and N. A. Kudryashov, On the Jacobi last multipliers and Lagrangians for a family of Liénard-type equations, *Appl. Math. Comput.* **307** (2017) 257–264.
28. Z. Liqin, Boundedness and convergence for the non-Liénard type differential equation, *Acta Math. Sci.* **27** (2007) 338–346.
29. G. G. Kiltu and G. F. Duressa, Accurate numerical method for Liénard nonlinear differential equations, *J. Taibah. Univ. Sci.* **13** (2019) 740–745.
30. P. T. Cardin and D. D. Novaes, Asymptotic behavior of periodic solutions in one-parameter families of Liénard equations, *Nonlin. Anal.* **190** (2020) 111617.
31. M. Cui and Y. Lin, *Nonlinear Numerical Analysis in the Reproducing Kernel Space* (Nova Science, USA, 2009).
32. A. Berlinet and C. T. Agnan, *Reproducing Kernel Hilbert Space in Probability and Statistics* (Kluwer Academic Publishers, USA, 2004).
33. A. Daniel, *Reproducing Kernel Spaces and Applications* (Springer, Basel, 2003).
34. O. Abu Arqub, Approximate solutions of DASs with nonclassical boundary conditions using novel reproducing kernel algorithm, *Fundam. Inform.* **146** (2016) 231–254.
35. W. Jiang and Z. Chen, A collocation method based on reproducing kernel for a modified anomalous subdiffusion equation, *Numer. Methods Partial Differ. Equ.* **30** (2014) 289–300.
36. F. Z. Geng, S. P. Qian and S. Li, A numerical method for singularly perturbed turning point problems with an interior layer, *J. Comput. Appl. Math.* **255** (2014) 97–105.

37. Y. Lin, M. Cui and L. Yang, Representation of the exact solution for a kind of nonlinear partial differential equations, *Appl. Math. Lett.* **19** (2006) 808–813.
38. Y. Zhoua, M. Cui and Y. Lin, Numerical algorithm for parabolic problems with non-classical conditions, *J. Comput. Appl. Math.* **230** (2009) 770–780.
39. A. Akgül, A novel method for a fractional derivative with non-local and non-singular kernel, *Chaos Solitons Fractals* **114** (2018) 478–482.